Physiological effects of inverse agonists in transgenic mice with myocardial overexpression of the β_2-adrenoceptor

Richard A. Bond*, Paul Leff†, T. David Johnson‡, Carmelo A. Milano§, Howard A. Rockman‖, Thomas R. McMinn‖, Subramaniam Apparsundaram*, Michael F. Hyek*, Terry P. Kenakin¶, Lee F. Allen# & Robert J. Lefkowitz☆**

* Department of Pharmacological and Pharmaceutical Sciences, University of Houston, Houston, Texas 77204, USA
† Department of Pharmacology, Fisons plc, Loughborough LE11 0RH, UK
‡ Department of Anesthesiology, Baylor College of Medicine, Houston, Texas 77030, USA
Departments of § Surgery, ☆ Cardiology and # Hematology/Oncology and the ☆ Howard Hughes Medical Institute, Duke University Medical Center, Durham, North Carolina 27710, USA
‖ Department of Medicine, University of California at San Diego, School of Medicine, La Jolla, California 92093, USA
¶ Glaxo Research, Research Triangle Park, North Carolina 27709, USA

G-PROTEIN-COUPLED receptors are thought to have an inactive conformation (R), requiring an agonist-induced conformational change for receptor/G-protein coupling[1–3]. But new evidence suggests a two-state model[4–19] in which receptors are in equilibrium between the inactive conformation (R), and a spontaneously active conformation (R*) that can couple to G protein in the absence of ligand (Fig. 1). Classic agonists have a high affinity for R* and increase the concentration of R*, whereas inverse agonists have a high affinity for R and decrease the concentration of R*. Neutral competitive antagonists have equal affinity for R and R* and do not displace the equilibrium, but can competitively antagonize the effects both of agonists and of inverse agonists. The lack of suitable *in vivo* model systems has restricted the evidence for the existence of inverse agonists to computer simulations[7,8] and *in vitro* systems[5,9–12,20–23]. We have used a transgenic mouse model in which there is such marked myocardial overexpression of β_2-adrenoceptors that a significant population of spontaneously activated receptor (R*) is present, inducing a maximal response without agonist[24]. We show that the β_2-adrenoceptor ligand ICI-118,551 functions as an inverse agonist, providing evidence supporting the existence of inverse agonists and validating the two-state model of G-protein-coupled receptor activation.

To assess inverse agonist effects, three lines of transgenic mice with cardiac-specific overexpression of the wild-type β_2-adrenoceptor[24] and control (non-transgenic) animals were investigated. Baseline atrial tension, assessed by isometric tension development in isolated left atria, was increased roughly threefold in transgenic lines with marked overexpression of the wild-type β_2-adrenoceptor (TG-4, TG-33)[24]. ICI-118,551, a β_2-adrenoceptor antagonist, inhibited baseline left atrial tension in these animals by 20–80% and the inhibitory effect correlated with β_2-adrenoceptor densities, that is, lines with higher receptor densities showed more inhibition (data not shown). This suggests that the inhibitory response to ICI-118,551 was receptor mediated and not a nonspecific event.

In atria from control mice, isoprenaline produced concentration-dependent increases in left atrial tension (Fig. 2*a*). The half-maximal effective concentration (EC_{50}) for isoprenaline in control mice (1.8×10^{-10} M) was shifted only fourfold to the right (7.7×10^{-10} M) by ICI-118,551, but 2,000-fold (3.9×10^{-7} M) in the presence of both ICI-118,551 and the β_1-adrenoceptor antagonist, CGP-20712A; the change in slope of the isoprenaline-response curve with ICI-118,551 results from the antagonist-induced conversion from a two-receptor- (β_1 and β_2-adrenoceptors) to a one-receptor- (β_2-adrenoceptor) mediated process. In transgenic animals, atrial tension is maximally stimulated at baseline and no response to isoprenaline was observed (Fig. 2*b*). Following ICI-118,551-induced inhibition of left atrial tension, however, isoprenaline increased left atrial tension, producing responses that restored this parameter to pre-antagonist values (Fig. 2*b*). In the presence of ICI-118,551, the EC_{50} for isoprenaline in transgenic atria (3×10^{-8} M) was shifted almost 170-fold when compared with its EC_{50} in control mice (1.8×10^{-10} M). No further shift was noted after the addition of CGP-20712A, indicating that functionally the response was mediated by a homogeneous population of β_2-adrenoceptors. To demonstrate the specificity of isoprenaline's ability to reverse the inhibitory effect of ICI-118,551, comparable reductions in baseline tension were produced using the cholinoceptor agonist, methacholine

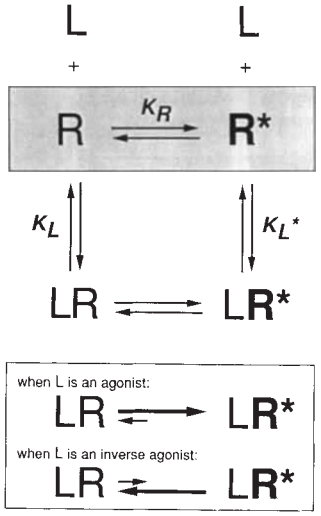

FIG. 1 The two-state model of receptor activation depicting the receptor existing in inactive (R) and active (R*) conformations; L, ligand; K_R, the equilibrium constant for the distribution of receptor between R and R* in the absence of ligand; K_L and K_{L^*}, the dissociation equilibrium constant for ligand at the two receptor states. These equilibria are defined as follows: $K_R = [R]/[R^*]$; $K_L = [R][L]/[LR]$; $K_{L^*} = [R^*][L]/[LR^*]$; and the total receptor population ($[R]_{TOT}$) $= [R] + [R^*] + [LR] + [LR^*]$. Using these equations, a relationship can be derived between the concentration of the agonist ([L]) and the concentration of receptors in the active form ($[R^*] + [LR^*]$), which is expressed as the fraction of the total receptor concentration (f_{R^*}) $= (K_{L^*} + [L])/K_{L^*}(1 + K_R) + (1 + K_R K_{L^*}/K_L)[L]$. The interactions between two ligands can be modelled by including the additional equilibrium equations, $K_B = [R][B]/[BR]$; $K_{B^*} = [R^*][B]/[BR^*]$, and extending the distribution equation[19]. Agonist concentration–response curves were simulated under two conditions: (1) the measured response is directly proportional to f_{R^*}, that is, with no receptor reserve; (2) the measured response is a rectangular hyperbolic function of f_{R^*}, that is, the fraction of receptors in the active state (f_{R^*}) required for a full response could be very small and therefore receptor reserve was present. In the latter case, an additional parameter, K_E is introduced, this being the value of f_{R^*} for half-maximal effect. Under this condition the difference between normal and TG-4 animals is modelled as a simple upregulation of receptor density; the absolute quantities of both R and R* increase, but the ratio remains the same. Under both conditions, the model fits the data equally well.

** Present address: Huntsman Cancer Institute, University of Utah, Health Sciences Center, Building 570, Room 410B, Salt Lake City, Utah 84112, USA.

(1 μM), or the calcium channel blocker, verapamil (100 nM). Under these conditions, isoprenaline was unable to reverse the inhibition of atrial tension by methacholine and only partially able (<50%) to reverse the inhibition by verapamil (data not shown). Conversely, if control mice were converted to a hypercontractile state (resembling TG-4 mice) through a non-β_2-adrenoceptor mechanism, that is, by increasing atrial tension with forskolin (10 μM), ICI-118,551 had no inhibitory effect (data not shown). These results indicate that the mechanism of ICI-118,551's inhibition of baseline atrial tension was through decreasing β-adrenoceptor-mediated increases in contractility.

If competition with endogenous catecholamines were the mechanism of ICI-118,551's inhibition, then any antagonist with affinity for the β_2-adrenoceptor used in the same relative concentration should produce an equal amount of inhibition. However, four different β-adrenoceptor antagonists, used at concentrations 300 times their K_B values (see Fig. 1) for the β_2-adrenoceptor[25], were found to produce widely varying degrees of inhibition of left atrial tension (alprenolol, propranolol, ICI-118,551 and nadolol produced 14±6%, 38±5%, 76±3% and 82±4% inhibition of baseline left atrial tension, respectively, data not shown). Treatment with the catecholamine-depleting agent, reserpine (0.3 mg per kg (body weight) intraperitoneally (ip), 24 h before killing) produced a >97% decrease in cardiac catecholamine content[26]. This dose of reserpine, however, did not affect baseline tension in the isolated atria of either TG-4 or control animals, and baseline responses in TG-4 animals remained comparable to the maximum response to isoprenaline in control animals (data not shown). In addition, the inhibitory concentration–response curve to ICI-118,551 (1×10^{-9} M to 3×10^{-6} M) was unaffected by reserpine treatment (data not shown). Thus, these experiments demonstrate that the inhibition of left atrial tension by ICI-118,551 does not result from antagonism of endogenous noradrenaline or adrenaline at the β-adrenoceptors.

The most conclusive evidence for the specificity of ICI-118,551's inhibition is provided by experiments assessing the net effect of the two β-adrenoceptor antagonists, ICI-118,551 and alprenolol. If the inhibitory effect of ICI-118,551 were due to either competition with endogenous noradrenaline or a non-specific effect, then the combination of these two antagonists should have exacerbated the effect, or at least left the larger effect intact. ICI-118,551 (1×10^{-9} M to 1×10^{-5} M) produced a concentration-dependent inhibition of baseline tension in the atria of TG-4 mice (Fig. 3*a*). The concentration–response curve for ICI-118,551 was displaced to the right by 30-fold (measured at the EC_{40}) by the competitive (neutral) antagonist alprenolol (1×10^{-7} M). This shift is consistent with alprenolol's known affinity for β_2-adrenoceptors[25] and is indicative of a competitive interaction between the two compounds for a single receptor site.

Experiments done in isolated atria with the β-adrenoceptor alkylating agent, pindobind, rule out a one-receptor-state model for receptor–ligand interactions. Pindobind (1×10^{-7} M for 15 min) decreased baseline tension of TG-4 atria by 25%. After pindobind treatment, the potency of ICI-118,551 increased with a 30-fold shift in the EC_{50} for ICI-118,551 to the left (Fig. 3*c*); this contrasts with a 30-fold decrease in the potency of isoprenaline after pindobind treatment of control animals (data not shown).

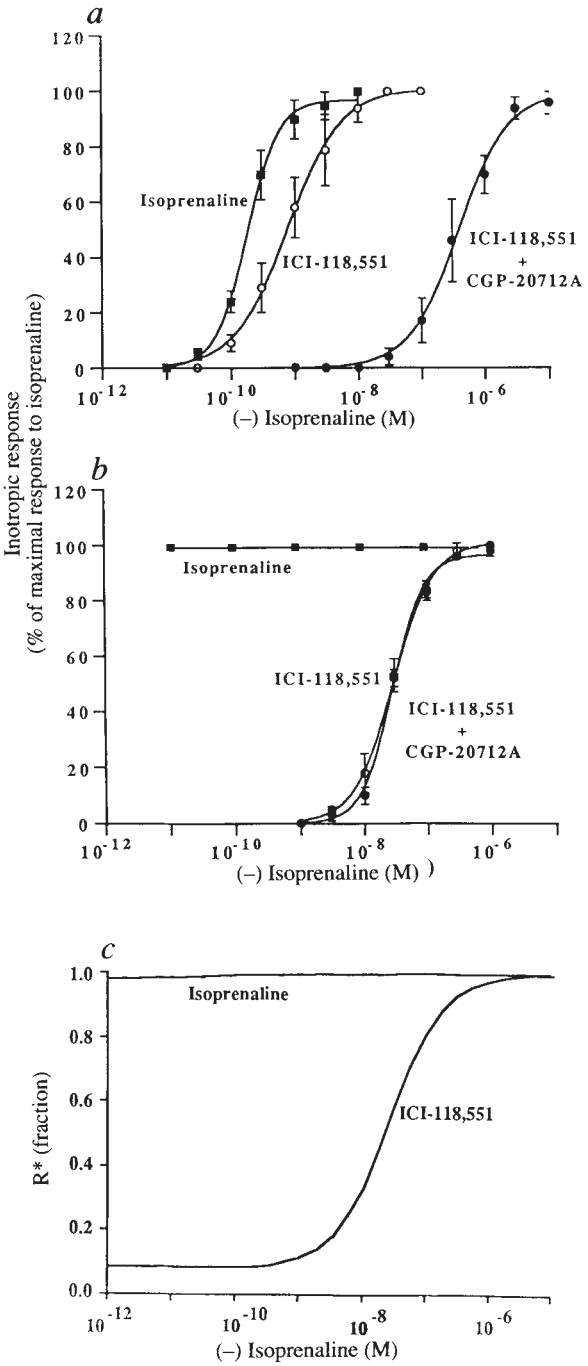

FIG. 2 The atria were suspended under optimal tension in modified Kreb's bicarbonate solution at 30 °C[24], and paced at the optimal frequency for tension development (3.2 Hz), 3 ms duration, voltage at threshold +20%; the results are expressed as the mean per cent inhibition ±s.e.m. ($n=4$ to 6 for each group); *a*, Left atrial tension development in response to isoprenaline in control and *b*, TG-4 mice. Isoprenaline concentration–response curve: control, ■; + ICI-118,551 (3×10^{-7} M), ○; +ICI-118,551 (3×10^{-7} M) and CGP-20712A (3×10^{-7} M), ●. Inotropic responses are expressed as the percentage of the maximal response to isoprenaline and data reported as the mean values ±s.e.m. ($n=8$ for control and $n=5$ for TG-4); baseline values for control and TG-4 mice were 83±10 mg and 262±42 mg, respectively. *c*, Simulation based on the simple form of the two-state model (no receptor reserve) using the following parameters; K_R (basal R/R^*) = 0.02; for isoprenaline, $K_L=1\times10^{-6}$ M, and $K_{L^*}=2\times10^{-9}$ M; for ICI-118,551, $K_L=5\times10^{-10}$ M, and $K_{L^*}=3\times10^{-6}$ M. Virtually identical simulations were obtained if receptor reserve was included (see legend to Fig. 1) using the same ligand parameter values, but with $K_R=10$ and $K_E=0.002$.

METHODS. Transgenic mice were produced using a transgene construct incorporating the alpha myosin heavy chain promoter ligated to the human β_2-adrenoceptor[24]; intense, cardiac-specific, overexpression of the adrenoceptor was achieved in these transgenic animals. Three lines overexpressing the wild-type β_2-adrenoceptor were investigated: TG-4, overexpressing the β_2-adrenoceptor at about 200 times the total cardiac β-adrenoceptor densities of control animals; TG-33, with receptor densities about 90-fold above control; TG-35, with densities about 50-fold above control[24].

Using the two-state model of receptor activation (Fig. 1), the interactions between isoprenaline and ICI-118,551 (Fig. 2*c*), ICI-118,551 and alprenolol (Fig. 3*b*), and ICI-118,551 and pindobind (Fig. 3*d*) were simulated. This was done using two different sets of assumptions, both of which yielded essentially the same results. In one set of simulations we assumed that receptor reserve characterized the system such that only a small fraction of activated receptors (f_{R^*}) was required for full response. Under these circumstances the high basal tension is explained without change in the receptor equilibrium simply by saturation of signal transduction processes by the increased tissue levels of R*. In the other set of simulations we assumed no receptor reserve and attributed the high basal tensions to a shift in the receptor state equilibrium towards R*. With both sets of assumptions isoprenaline was unable to evoke a further response (control curve). In both cases, the effects of ICI-118,551 were modelled assuming that this ligand functions as an inverse agonist, displacing receptors back towards the inactive form (R). Under this condition, isoprenaline could now evoke a full response in TG-4 tissues (Fig. 2*c*). The simulation(s) parallels the experimental data, demonstrating that the model can accurately account for this ligand interaction. Likewise, the concentration–response curve of ICI-118,551 could be simulated using the two-state model assuming alprenolol had equal affinity for the two receptor states (Fig. 3*b*) with good correspondence between the simulation(s) and the experimental data. Pindobind lowered baseline tension and markedly shifted the ICI-118,551 concentration–response curve to the left. These effects were simulated assuming that pindobind alkylates both receptor states equally, causing a reduction in the total receptor population without a change in the ratio. This decreases R* to a level below that which saturates signal transduction processes and accounts for the decrease in basal tension produced by pindobind. Because there is also less functional opposition to the inverse agonist effects of ICI-118,551, its curve is left-shifted. An identical simulation could be achieved without the assumption of receptor reserve, but this involved the perhaps unnecessarily speculative assumption that pindobind is able to alter K_R. In both cases, the model provided a good fit (Fig. 3*d*) to the experimental data.

To assess the effect of ICI-118,551 and alprenolol on left ventricular performance *in vivo*, the maximum first derivative of the left ventricular systolic pressure (LV dP/dt_{max}), an index of cardiac contractility, was measured in TG-4 and control mice[24]. In TG-4 animals, ICI-118,551 reduced LV dP/dt_{max} by about

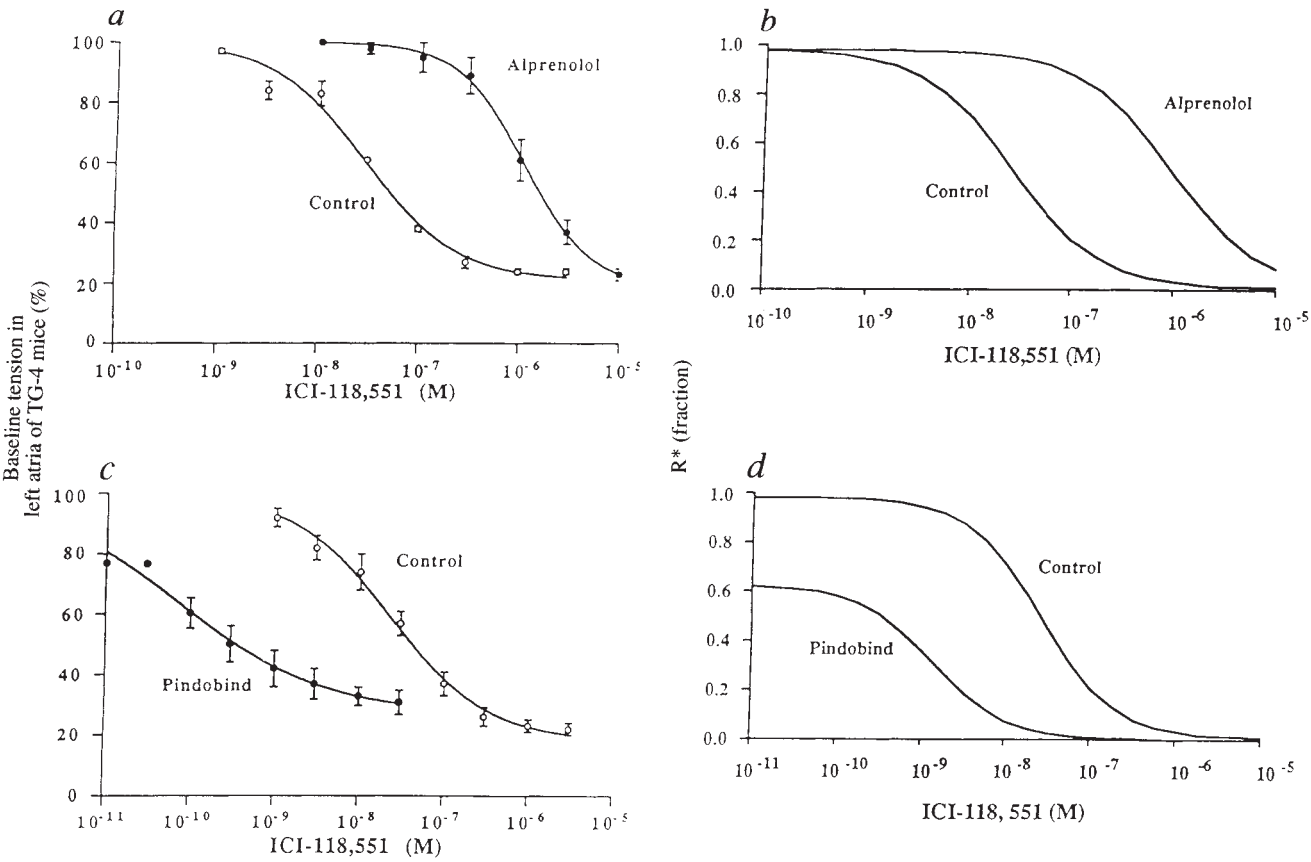

FIG. 3 *a*, The effect of alprenolol on the inhibitory response of ICI-118,551 on baseline left atrial tension in TG-4 mice; control, ○; alprenolol (1×10^{-7} M), ●. The results are expressed as the mean per cent inhibition of baseline ±s.e.m. (baseline ± s.e.m. = 271 ± 35 mg; $n = 5$ for ICI-118,551 alone; and 223 ± 40 mg; $n = 5$ for ICI-118,551 in the presence of alprenolol). *b*, Simulation based on the simple form of the two-state model using the following parameters; K_R (basal R/R*) = 0.02; for ICI-118,551, $K_L = 5 \times 10^{-10}$ M, and $K_{L^*} = 3 \times 10^{-6}$ M; alprenolol was defined as a neutral competitive antagonist, $K_L = K_{L^*} = 3 \times 10^{-9}$ M (based on a pA_2 (−log K_B) value of 8.5 (ref. 25)). Incorporating receptor reserve (see legend to Fig. 1), virtually identical simulations were obtained using the same ligand parameters and $K_R = 10$ and $K_E = 0.002$. *c*, The effect of pindobind (1×10^{-7} M, 15 min incubation) on the inhibitory response of ICI-118,551 on baseline left atrial tension in TG-4 mice; control, ○; pindobind, ●. *d*, Simulation based on the two-state model using the following parameters; K_R (basal R/R*) = 0.02; for ICI-118,551, $K_L = 5 \times 10^{-10}$ M, and $K_{L^*} = 3 \times 10^{-6}$ M; pindobind was assumed to alter K_R (basal R/R*) from 0.02 to 0.6 as a result of preferential enrichment of R. Virtually identical simulations were obtained including receptor reserve using the same ligand parameters and $K_R = 10$ and $K_E = 0.002$. In this case, pindobind was assumed to reduce the absolute value of R and R* equally by 30-fold as a result of receptor alkylation. Experimentally, ICI-118,551 produced a maximum decrease in tension of 80%, and for the simulations, it was assumed that this value represented full inverse agonism. To allow side-by-side comparison of the theoretical and experimental graphs, the *y*-axes of the simulations were scaled to this range.

70% after 4 min (Fig. 4*a*) with more profound decreases after longer treatment periods (data not shown). This was associated with a fall in heart rate (485 ± 13 to 336 ± 17 b.p.m.) and a fall in LV systolic pressure (74 ± 2 to 54 ± 6 mm Hg) (data not shown). ICI-118,551 had no effect on LV dP/dt_{max} in control animals (data not shown). Alprenolol produced only a 25% decrease in LV dP/dt_{max} (Fig. 4*a*) with no further effect after 4 min, and no significant effects on either heart rate or LV systolic pressure. In addition, pre-treatment with alprenolol significantly blocked the effects of ICI-118,551 on LV dP/dt_{max} (Fig. 4*a*) as well as heart rate and LV systolic pressure.

The effect of ICI-118,551 and alprenolol on adenylyl cyclase activity was also examined in cardiac membranes[24]. β-Adrenoceptor stimulation increases adenylyl cyclase activity, increasing intracellular cAMP and contractility; baseline levels of adenylyl cyclase were elevated in transgenic animals[24]. Comparable to the results obtained in isolated atria and *in vivo*, alprenolol could antagonize the inhibitory effect of ICI-118,551 on adenylyl cyclase activity (Fig. 4*b*); co-incubation of both antagonists resulted in a significant attenuation of the effect of ICI-118,551 alone.

These experiments suggest that the myocardium of transgenic mice contains a markedly elevated number of wild-type β_2-adrenoceptors in the active conformation (R*), which can therefore increase adenylyl cyclase activity and enhance left atrial tension and left ventricular contractility. These findings provide physiological support for a model of receptor action which predicts that receptors exist in an equilibrium between two allosterically different conformations (Fig. 1), R and R* (refs 5, 11–17). In addition, these data demonstrate that ICI-118,551 functions as an inverse agonist, presumably, by shifting the equilibrium between R and R* towards the inactive conformation (R).

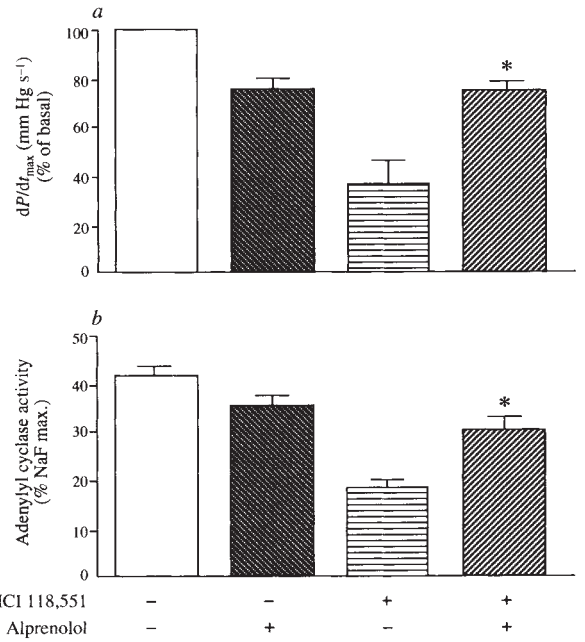

FIG. 4 *a*, The effect of ICI-118,551 and alprenolol on the *in vivo* measurement of LV dP/dt_{max}[24] in TG-4 mice. LV dP/dt_{max} in TG-4 mice ($n=7$) before and 4 min after the administration of ICI-118,551 (5 μg i.v.) or alprenolol (10 μg i.v.); at 6 min (data not shown), all animals treated with ICI-118,551 became hypotensive and developed severely depressed LV dP/dt_{max}. The effect of ICI-118,551 on LV dP/dt_{max} in TG-4 animals pretreated with alprenolol 4 min before the administration of ICI-118,551 ($n=8$); *, the inhibitory effect of ICI-118,551 was significantly attenuated by alprenolol pretreatment, $P<0.05$. Data are reported as the mean ±s.e.m. *b*, The effect of ICI-118,551 (1×10^{-7} M) and alprenolol (1×10^{-6} M) on adenylyl cyclase activity[24] in membranes prepared from TG-4 hearts; *, differs from response in the presence of ICI-118,551 alone, $P<0.05$. All responses are expressed as a percentage of the maximal stimulation by NaF (10 mM) ($n=4$ or 5 per group).

Using equations based on a simple two-state model of receptor activation (Fig. 1), the interaction between the effects of the inverse agonist, ICI-118,551, and the agonist isoprenaline (Fig. 2*c*) or the competitive (neutral) antagonist alprenolol (Fig. 3*b*) could be quantitatively modelled. The striking correlation between the simulations and the experimental data demonstrates that this model accurately predicts the behaviour of ligands in this system. In accepting the theoretical analysis of the data, the choice of parameter values used is important and it should be emphasized that the values of K_L and K_{L^*} for ICI-118,551, and the value of the basal ratio of R/R^* (K_R) were the same in each of the three simulations.

Classical receptor theory has as its cornerstone the occupancy–response relationship[1–3], that is, the magnitude of the response obtained is directly proportional to the number of receptors occupied by ligand. The increased potency of the inverse agonist response after receptor alkylation by pindobind, however, is irreconcilable with a single-state receptor model for occupancy–response. The simulations using the two-state model accurately predict the effects of pindobind on ICI-118,551 response curves.

The prevailing concept of ligand efficacy for G-protein-coupled receptors may now need to be carefully re-examined. With the development of sensitive test systems for the detection of inverse agonism, such as these transgenic animals, many pharmacological agents may need reclassification. If ligand efficacy is the differential affinity of a ligand for the two existing conformations of the receptor, then an expectation of 'zero' efficacy, which would be required of a pure neutral antagonist, may be relatively uncommon, because this would require identical drug affinities for both receptor states[11,12]. Numerous drugs previously classified as neutral antagonists, therefore, may actually function as inverse agonists[11,12,15,16,21,22], and such a reclassification would have important pharmacological and therapeutic implications.

These studies also highlight the important potential for inverse agonists in drug development as new, targeted therapeutic agents. In addition to eliminating tonic endogenous agonist tone like the neutral antagonists, inverse agonists can also negate constitutive receptor activity; this may be particularly important in disease states that result from constitutively activating receptor mutations. The development of thyroid adenomas and male precocious puberty[27,28] are two examples of such human diseases in which receptor mutants play a role in disease pathogenesis by inducing constitutive activity. Potentially these compounds would also have applicability in diseases resulting from receptor overexpression, such as the dopamine D_4 receptor in schizophrenia[29]; such overexpression can induce a constitutively active phenotype[24] and make the disease resistant to standard antagonists. Inverse agonists, therefore, may represent an important and specific therapeutic approach for such disease states. □

Received 3 June 1994; accepted 16 January 1995.

1. Clark, A. J. in *The Mode of Action of Drugs on Cells* (Edward Arnold, London, 1933).
2. Ahriens, E. J. *Arch Int. Pharmacodyn.* **99,** 32–49 (1954).
3. Stephenson, R. P. *Br. J. Pharmacol.* **11,** 379–393 (1956).
4. De Lean, A., Stadel, J. M. & Lefkowitz, R. J. *J. biol. Chem.* **255,** 7108–7117 (1980).
5. Samama, P., Cotecchia, S., Costa, T. & Lefkowitz, R. J. *J. biol. Chem.* **268,** 4625–4636 (1993).
6. Ehlert, F. J. *Trends pharmacol. Sci.* **7,** 28–32 (1986).
7. Costa, T., Ogino, Y., Munson, P. J., Onaran, O. & Rodbard, D. *Molec. Pharmacol.* **41,** 549–560 (1992).
8. Onaran, H. O., Costa, T. & Rodbard, D. *Molec. Pharmacol.* **43,** 245–255 (1992).
9. Costa, T. & Herz, A. *J. Proc. natn. Acad. Sci. U.S.A.* **86,** 7321–7325 (1989).
10. Costa, T., Lang, J., Gless, C. & Herz, A. *Molec. Pharmacol.* **37,** 383–394 (1990).
11. Samama, P., Pei, G., Costa, T., Cotecchia, S. & Lefkowitz, R. J. *Molec. Pharmacol.* **45,** 390–394 (1994).
12. Chidiac, P., Hebert, T. E., Valiquette, M., Dennis, M. & Bouvier, M. *Molec. Pharmacol.* **45,** 490–499 (1994).
13. Lefkowitz, R. J., Cotecchia, S., Samama, P. & Costa, T. *Trends pharmacol. Sci.* **14,** 303–307 (1993).
14. Schutz, W. & Freissmuth, M. *Trends pharmacol. Sci.* **13,** 376–380 (1992).

15. Mewes, T., Dutz, S., Ravens, U. & Jakobs, K. H. *Circulation* **88,** 2916–2922 (1993).
16. Gotze, K. & Jakobs, K. H. *Eur. J. Pharmacol.* **268,** 151–158 (1994).
17. Monod, J., Wyman, J. & Changeux, J-P. *J. molec. Chem.* **12,** 88–118 (1965).
18. Colquhoun, D. in *Drug Receptors* 149–181 (MacMillan, London, 1973).
19. Leff, P. *Trends pharmacol. Sci.* (in the press).
20. Cerione, R. A *et al. Biochemistry* **23,** 4519–4525 (1984).
21. Senogles, S. E. *et al. J. biol. Chem.* **262,** 4860–4867 (1987).
22. Barker, E. L., Westphal, R. S., Schmidt, D. & Sanders-Bush, E. *J. biol. Chem.* **269,** 11687–11690 (1994).
23. Tian, W-N., Duzic, E., Lanier, S. M. & Deth, R. C. *Molec. Pharmacol.* **45,** 524–531 (1994).
24. Milano, C. A. *et al. Science* **264,** 582–586 (1994).
25. Arch, J. R. S. & Kaumann, A. J. *Mednl Res. Rev.* **13,** 663–729 (1993).
26. Schwartz, D. D. & Eikenburg, D. C. *J. Pharmacol. exp. Ther.* **244,** 11–18 (1988).
27. Shenker, A. *et al. Nature* **365,** 652–654 (1993).
28. Parma, J. *et al. Nature* **365,** 649–651 (1993).
29. Seeman, P., Guan, H-C. & Van Toi, H. H. M. *Nature* **365,** 441–445 (1993).

ACKNOWLEDGEMENTS. We thank D. Eikenburg for his support and critical review of this manuscript and M. Holben and D. Addison for secretarial assistance.

Replication of transcriptionally active chromatin

Renzo Lucchini & José M. Sogo

Institute of Cell Biology, Swiss Federal Institute of Technology, ETH-Hönggerberg, CH-8093 Zürich, Switzerland

In eukaryotic cells, active genes and their regulatory sequences are organized into open chromatin conformations in which nucleosomes can be modified, disrupted or totally absent[1–3]. It has been proposed that these characteristic chromatin structures and their associated factors might be directly inherited by the newly synthesized daughter strands during chromosome duplication[4–6]. Here we show that in the yeast *Saccharomyces cerevisiae*, replication machinery entering upstream of a transcriptionally active ribosomal RNA gene generates two newly replicated coding regions regularly packaged into nucleosomes, indicating that the active chromatin structure cannot be directly inherited at the replication fork. Whereas the establishment of an exposed chromatin conformation at some newly replicated rRNA gene promoters can occur shortly after the passage of the replication fork, regeneration of the active chromatin structure along the coding region is always a post-replicative process involving disruption of preformed nucleosomes.

We have previously shown that in a growing yeast cell only a fraction of the ~150 tandemly repeated rRNA genes are transcriptionally active[7]. Active and inactive copies can be distinguished by their different accessibility *in vivo* to the intercalating drug psoralen, which can introduce crosslinks into DNA sites that are not protected by nucleosomes[3,8]. In this assay, each rRNA coding fragment is separated into two distinct bands on native agarose gels: a slowly migrating band representing highly crosslinked DNA derived from transcriptionally active genes organized in a heavily disrupted chromatin structure, and a fast-migrating band containing slightly crosslinked DNA originating from the inactive, nucleosome-packed gene copies[9,10] (s and f bands in Fig. 1, lanes L).

To study the chromatin structure of newly replicated DNA, we analysed the extent of crosslinking of rRNA coding fragments excised from the replicated branches of replication intermediates purified from preparative two-dimensional gels[11]. Figure 1*b* (lane 3) shows an analysis of the 1.9-kilobase (kb) *Eco*RI-digested coding fragment derived from the replicated sections of gel-purified replication intermediates (shaded portions of fork 3 in Fig. 1*a*), in which there is only one band with the same mobility as the slightly crosslinked, fast-migrating band (for exponentially growing cells, see Fig. 1*d*). On the other hand, the proportion of the s and f bands generated by a fragment derived from the unreplicated portion of early replication intermediates eluted from the same two-dimensional gel is consistent with the presence of a large fraction of replicating molecules having parental DNA sequences organized in an active chromatin structure (Fig. 1*c*, lane 1). These results indicate that the replication machinery always generates two newly replicated coding regions tightly packaged in nucleosomal arrays.

To examine chromatin structure at the replication forks in more detail, we analysed single DNA replication intermediates by electron microscopy[3,12]. The nucleosomal intergenic spacer is visualized as a row of single-stranded bubbles, whereas highly crosslinked DNA derived from transcriptionally active genes has a double-stranded appearance[7] (Fig. 2*a*). In the rDNA repeats shown in Fig. 2*b* and *c*, a replication fork has entered the upstream gene. Whereas the unreplicated parental DNA immediately ahead of the fork is fairly continuously crosslinked, the newly replicated coding sequences are oganized as rows of single-stranded bubbles, consistent with the presence of nucleosomes (see also Fig. 2*d*). Measurements of the length of the short nucleosome-free region immediately behind the replication

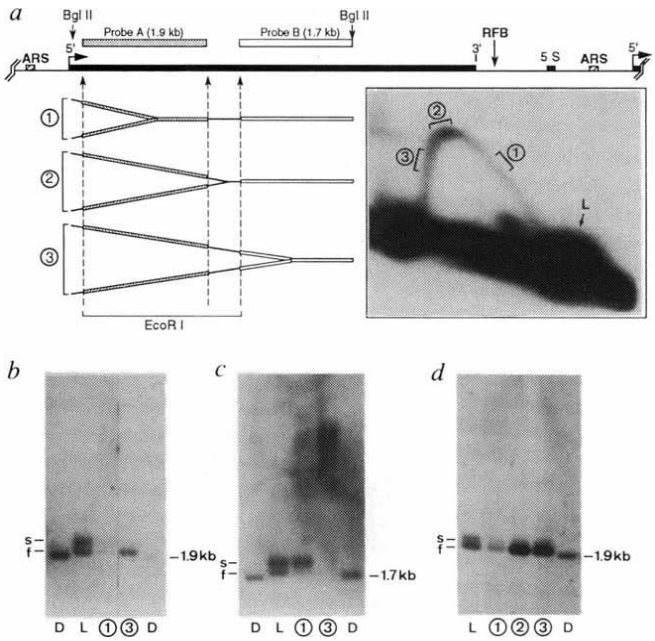

FIG. 1 Psoralen accessibility of replicating rRNA coding fragments. *a*, Map showing the structural organization of the rDNA repeat unit of *S. cerevisiae*. The 35S precursor coding region is indicated as a filled box. In the rRNA intergenic spacer, the replication fork barrier (RFB), the 5S rRNA gene (5S) and the autonomously replicating sequence (ARS) are shown. Probes A and B detect the 1.9-kb *Eco*RI and the 1.7-kb *Eco*RI–*Bgl*II fragments, respectively, derived from the tandemly repeated rRNA coding regions. The autoradiograph below the map shows rDNA from psoralen crosslinked S-phase cells which has been digested with *Bgl*II, separated on a 2D gel, blotted and hybridized with probe A. The position of the linear 4.5-kb *Bgl*II coding fragment is indicated by the arrow (L). As in yeast most of the rRNA genes are replicated in the same direction as transcription[14], most of the Y-shaped replication intermediates of this coding fragment migrating in regions 1, 2 and 3 of this arc have the same structure and orientation as those of forks 1, 2 and 3 (shown on the left), respectively. *b*, rDNA isolated from regions L, 1 and 3 of a 2D gel similar to that shown in *a*, was digested with *Eco*RI, separated on a 1.5% agarose gel, blotted and hybridized with probe A. Lane D: non-crosslinked control DNA digested with *Eco*RI. *c*, Aliquots of the same samples as used in *b* were separated on the same gel, blotted and hybridized with probe B. *d*, Similar experiment as in *b*, except that the rDNA was isolated from psoralen-crosslinked exponentially growing cells.
METHODS. *S. cerevisiae* A1 cells (*MATa* ade2-101 ura3-52 his3Δ200 lys2-801 Δbar1::LYS2) were grown, shyncronized, and photoreacted as described[11]. Crosslinked rDNA was purified on a CsCl–actinomycin D gradient[7]. Preparative 2D-gel electrophoresis, transfer and hybridization were done as described[11].